DOI 10.1007/s10812-020-00954-y
Journal of Applied Spectroscopy, Vol. 87, No. 1, March, 2020 (Russian Original Vol. 87, No. 1, January–February, 2020)

STRUCTURE OF PHOTOLUMINESCENCE SPECTRA OF OXYGEN-DOPED GRAPHITIC CARBON NITRIDE

E. B. Chubenko,[a*] A. V. Baglov,[a] M. S. Leonenya,[b] G. P. Yablonskii,[b] and V. E. Borisenko[a,c]

UDC 535.37:547.491.8

The relationships governing variation of the photoluminescence of graphitic carbon nitride synthesized by heat treatment of melamine in a closed air medium containing oxygen in the temperature range of 10–300 K were investigated. It was shown that the concentration of oxygen in the obtained material 4–5 at.% increases with increase of temperature and decreases with increase in the duration of the synthesis process. By measurements at reduced temperatures right down to 10 K it was possible to resolve bands due to radiative recombination processes in the photoluminescence spectra of the graphitic carbon nitride. It was found that increase of the synthesis temperature from 500 to 600°C and also increase of the duration at the given temperature from 30 to 240 min shift the maximum in the photoluminescence spectrum from 2.74 eV into the region of lower energies to 2.71–2.67 eV. This is due to the bigger role of the molecular system formed by the π bonds of carbon and nitrogen atoms with sp^2 hybridization and characterized by a smaller forbidden band width in the emission of light. Transitions due to recombination through oxygen-induced levels in the forbidden band of the semiconductor lead to the appearance of a "tail" in the photoluminescence spectra in the region of low energies (2.40–2.33 eV). Increase of the carbon nitride synthesis temperature to 600°C leads to a change in the structure of the energy bands and to increase of the energy of the radiative transitions as a result of increase in the degree of doping with oxygen atoms and thermal stratification.

Keywords*: carbon nitride, melamine, photoluminescence.*

Introduction. Among polymorphous modifications of compounds consisting of nitrogen and carbon atoms graphitic carbon nitride (*g*-C_3N_4) is the most stable under normal conditions [1–3]. The ideal structure of this material represents molecules of tri-sym-triazine (heptazine) linked to each other by amino groups and forming two-dimensional sheets linked to each other by van der Waals forces in the way that sheets of graphene form the structure of graphite [3–7]. In fact, *g*-C_3N_4 can be regarded as a polymeric semiconductor the monomer of which is the heptazine molecule; it is insoluble in water and most organic solvents, has high chemical stability in acidic and alkaline mediums, and is thermally stable up to 700°C [3, 8]. The bright photoluminescence (PL) at room temperature in the optical region of wavelengths and the marked photocatalytic effect [8–10] are of considerable scientific and practical interest in the development of technology for synthesis of this material and investigation of its properties. Moreover, *g*-C_3N_4 may find use in optoelectronics, photovoltaics, and "green" energy as a material for photocatalytic coatings in effluent purification and the synthesis of hydrogen fuel [8, 11–13]. The principal method for the production of *g*-C_3N_4 is pyrolytic decomposition of various precursors followed by thermal condensation and polymerization [3, 8, 11].

The precursors most widely used in practice are melamine, urea, thiourea, cyanamide, and dicyanamide [11]. It is not possible to obtain *g*-C_3N_4 with ideal crystal structure by the pyrolytic method on account of the so-called kinetic limitations, which depend on the fact that losses of carbon occur during the synthesis as a result of the formation of volatile carbon-containing compounds [14]. The stoichiometric ratio C/N = 0.75 is not therefore attained in practice. The *g*-C_3N_4 is not usually a fully polymerized material and contains residual hydrogen (up to 2 wt.%), amino groups, structural defects, and broken bonds [15]. It is interesting that the photocatalytic characteristics of *g*-C_3N_4 with ideal crystal structure are

*To whom correspondence should be addressed.

[a]Belarusian State University of Informatics and Radioelectronics, Minsk, 220013, Belarus; email: eugene.chubenko@gmail.com; [b]B. I. Stepanov Institute of Physics of the National Academy of Sciences of Belarus, Minsk, 220072, Belarus; [c]National Research Nuclear University MEPhI, Moscow, 115409, Russia. Translated from Zhurnal Prikladnoi Spektroskopii, Vol. 87, No. 1, pp. 14–20, January–February, 2020. Original article submitted October 20, 2019.

significantly inferior to those in the material with a high concentration of defects [7, 16] because it is the latter that promote the photocatalytic reactions on its surface.

The structure of g-C_3N_4 and the concentration of impurities in it are affected by the condensation temperature, the concentration of the precursor, the after treatment, and doping [3, 7]. Changes in the structural characteristics of g-C_3N_4 are reflected in its optical characteristics and can be analyzed indirectly by changes in the PL spectra [7, 17]. Most of the papers on g-C_3N_4 at the present time have concentrated on investigation of its photocatalytic properties [3, 8, 10, 18]. However, the authors know of a few publications in which the relationships linking changes in the photoluminescence characteristics of g-C_3N_4, its band structure, and the conditions of synthesis have been analyzed [17, 19–24]. It was shown that increase in the degree of polymerization of a semiconducting compound with increase of synthesis temperature shifts the PL maximum into the long-wave region of the spectrum. In [25] it was noticed that with increase in the temperature of g-C_3N_4 the PL maximum is shifted into the region of higher photon energies in agreement with the empirical equation of Varshni [26], which describes the temperature behavior of the forbidden band width of semiconductors. The forbidden band width of g-C_3N_4 is estimated to lie in the region of 2.70–2.88 eV at 300 K [3, 19, 20, 23]. In [24] the structure of the PL and PL excitation spectra recorded at room temperature for g-C_3N_4 synthesized at 400–700^{o}C was analyzed. Breakdown of the spectra into components in the form of Gaussian functions showed that several radiative recombination processes occur simultaneously in g-C_3N_4. However, the breakdown was not precise, and certain visible spectral maxima were not accounted for. Lowering of the temperature of the PL measurements should make it possible to resolve individual bands associated with various radiative recombination processes in g-C_3N_4. The main object of the present work was to study the effect of the conditions for synthesis of g-C_3N_4 from melamine at 500–600^{o}C and its length on PL in the temperature range of 10–300 K.

Experimental. Bulk g-C_3N_4 was synthesized by pyrolytic decomposition of melamine followed by polymerization of the products in a closed atmosphere by the method in [21, 22]. A 2-g sample of the powdered precursor was placed in a 20-mL ceramic crucible which was then sealed mechanically and placed in a muffle furnace for heat treatment at a fixed temperature in the range of 500–600^{o}C for 30–240 min. The heating rate was 5^{o}C/min. The crucible was cooled gradually for up to 12 h.

The presence of a crystalline phase of g-C_3N_4 in the synthesized material was established by x-ray structure analysis (source CuK_α line 1.54179 nm). The elemental composition was determined by x-ray energy dispersive analysis with a Bruker QUANTAX 200 spectrometer. Photoluminescence was excited at temperatures in the region of 10–300 K by the radiation of an He–Cd laser (λ = 325 nm) with the sample placed in a closed-cycle helium cryostat. The excitation power density level at the surface of the sample was ~0.1 W/cm^2. The luminescence spectra were recorded on a Solar LS SDH-VI spectrometer.

Results and Discussion. As in previous investigations with thiourea as precursor [21], it was possible by heat treatment of melamine to obtain powders of characteristic yellow color [3] having the structure of g-C_3N_4 as confirmed by the results of x-ray structure analysis. According to the data from x-ray energy dispersive analysis (Table 1), the concentration of oxygen atoms in the g-C_3N_4 synthesized a 500^{o}C was lower than in the material synthesized at 600^{o}C, but the ratio of atomic concentrations of carbon and nitrogen was larger and close to stoichiometric (C_C/C_N = 0.75). If the length of the process is increased to 240 min the atomic concentration of oxygen (C_O) in the g-C_3N_4 is reduced by 0.1–0.2 at.%. At 500^{o}C the C_C/C_N ratio in the obtained material is higher with greater process productivity, but at 600^{o}C it is lower.

The PL spectra of the g-C_3N_4 powders synthesized for various process times at various temperatures (Fig. 1) have a wide structured band in the region of 3–2 eV at temperatures 10–300 K. Such detail in the PL spectra was not found in [24]. By breaking the PL spectra down into components having the form of a symmetrical Gaussian distribution it was possible to determine the position of their maxima and their full width at half maximum (FWHM) (Table 2).

The obtained data show that increase of the temperature of the powder shifts the maximum of the bands into the region of lower energies and increases their width at half height. The contribution from the individual bands to the integral PL intensity changes with variation of the temperature of the sample. The intensity of bands I and II, corresponding to the higher energies, decreases whereas the intensity of the low-energy transitions (III and IV) increases somewhat. The largest changes in the form of the PL spectrum and the intensity of the individual bands are observed for the g-C_3N_4 sample obtained at T = 600^{o}C. At T = 10 K an additional band V with a maximum at 3.074 eV appears in the PL spectrum of this sample in the region of high energies. With increase of synthesis temperature from 500 to 600^{o}C the relative integral intensity of the PL spectrum decreases by ~4 times. The same occurs if the duration of the synthesis process is increased to 240 min.

The integral intensity of the PL spectrum for all the bands (Fig. 1, inset) also decreases with decrease of the measurement temperature. The PL spectrum becomes smoother, and at room temperature (300 K) the individual PL bands

TABLE 1. Elemental Composition of g-C_3N_4 Powders Obtained at Various Temperatures (T) and Synthesis Times (t)

T, °C	t, min	C_C/C_N	C_O, at.%
500	30	0.56	4.45
	240	0.57	4.25
600	30	0.59	4.64
	240	0.54	4.51

TABLE 2. Position of the Maxima (E, eV) and the Width at Half Maximum (FWHM, nm) of Components I–V of the Structured Photoluminescence Band of the g-C_3N_4 Sample Obtained at Various Temperatures and Synthesis Times

Sample synthesis regime (T, t)	I		II		III		IV		V	
	E	FWHM	E	FWHM	E	FWHM	E	FWHM	E	FWHM
T = 10 K										
500°C, 30 min	2.828	19.03	2.706	30.02	2.576	58.40	2.406	105.63	–	–
500°C, 240 min	2.819	20.26	2.699	34.57	2.541	61.81	2.337	109.216	–	–
600°C, 30 min	2.894	30.71	2.734	35.90	2.561	60.93	2.399	124.72	3.074	12.79
T = 300 K										
500°C, 30 min	2.82	21.2	2.706	32.74	2.565	59.84	2.379	110.16	–	–
500°C, 240 min	2.8	24.74	2.679	34.07	2.523	61.46	2.33	117.26	–	–
600°C, 30 min	2.83	24.51	2.717	40.49	2.517	85.7	2.338	165.63	–	–

become broader and merge into a single broad band. This resultant band is usually recorded during investigation of the photoluminescence of g-C_3N_4 [17, 19–25].

The presence of oxygen atoms in the obtained material is due to the fact that the synthesis of g-C_3N_4 occurs in air containing oxygen, which reacts with the intermediate reaction products and is included in the structure of the obtained product in the process that leads to the formation of melon and g-C_3N_4 [27]. As the synthesis temperature increases with a short process time (30 min) the ratio of carbon to nitrogen atoms (CC/CN) increases, indicating a greater degree of polymerization of the material since the decrease in the relative concentration of nitrogen is due to the elimination of amino groups and the formation of chemical bonds between the heptazine molecules [7]. The CC/CN ratio also increases when synthesis process at 500°C is longer (up to 240 min) since a larger number of heptazine molecules and polymer chains of melon are able to form chemical bonds with each other, and the formed polymeric semiconductor gradually solidifies, i.e., its degree of polymerization increases. At a high synthesis temperature (600°C) increase of the time leads to decrease of the C_C/C_N ratio since elimination of the amino groups and polymerization of the material under such conditions begin to compete with the thermal decomposition of the g-C_3N_4 with the release of carbon compounds [14]. With a long synthesis time the amount of amino groups decreases and the polymerization process becomes slower, but the thermal decomposition process is only related to temperature and continues to occur at the same rate, and it is this that leads to the observed decrease of the C_C/C_N ratio. The increase in the concentration of oxygen with increase of synthesis temperature may be due to the higher reactivity of the material when the total energy of the system is higher. The decrease of the oxygen concentration with increase in the length

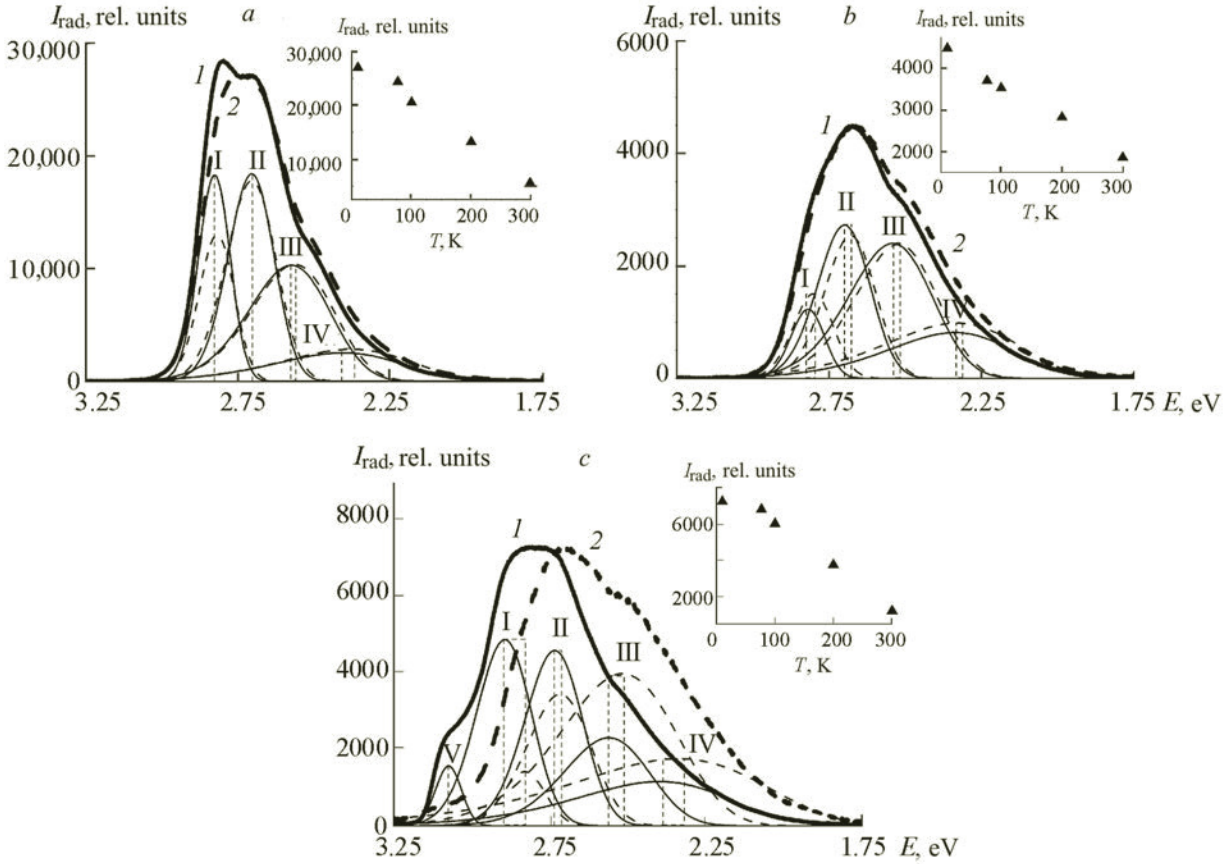

Fig. 1. Intensity normalized low-temperature (1) and high-temperature (2) PL spectra of g-C_3N_4 and the corresponding bands I–IV; synthesis at 500°C and duration 30 min (a), 500°C and 240 min (b), and 600°C and 30 min (c); insets, dependence of spectral integral PL intensity on sample temperature.

of the synthesis process is due thermal decomposition, evaporation of the oxygen-containing compounds, and the limited amount of free oxygen in the closed volume of the crucible.

The simplified band structure of g-C_3N_4 is presented in Fig. 2. The valence band of the polymeric semiconductor is formed by the C–N σ bonds with sp^3 hybridization (σ level), the C–N π bonds with sp^2 hybridization (π level), and the unshared electron pairs of nitrogen (UP level N_2). The conduction band is formed by excited σ and π bonds (denoted as σ^* and π^*). In the forbidden band of g-C_3N_4 there are also impurity levels coupled with the oxygen atoms and the structural defects of the material [19, 28].

The bands observed in the PL spectra of g-C_3N_4 produced at 500°C with a process rime of 30 min are due to permitted radiative transitions between the σ^* and UP levels of N_2 (band I) [17, 24], the π^* and UP levels of N_2 (band II) [17, 24], transitions between the levels of defects associated with the nitrogen (C≡N triple bonds, NH_2 groups, vacancies), and UP N_2 orbitals (band III) [19, 24], and the transitions of electrons to levels due to doping of the g-C_3N_4 with oxygen (band IV) [17, 19, 28]. The large width of the last band is due to dispersion of the energy of possible radiative transitions to the impurity levels of oxygen. The red shift of the maxima of the PL bands with increase of measurement temperature is due to temperature blurring of the energy bands and to actual narrowing of the forbidden band of the material. The decrease of the PL intensity with increase of temperature is explained by thermal activation of the channels of nonradiative recombination associated with surface states, impurities, and defects.

If the length of the synthesis of g-C_3N_4 is increased to 240 min the degree of polymerization increases (this is confirmed by the C/N ratio), and the density of the material rises, leading to an increase in the number of C–N π bonds with sp^2 hybridization. Here the probability of relaxation of the excited photoelectrons from the σ^* to the π^* level followed by radiative transitions to the UP level of N_2 is increased. With increase in the length of the synthesis of g-C_3N_4, therefore, the

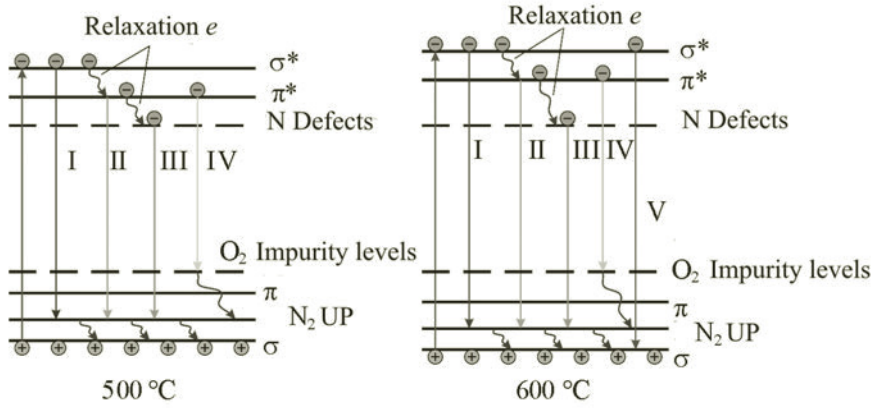

Fig. 2. Structure of the g-C_3N_4 energy bands with indication of possible radiative and nonradiative transitions between the levels at various temperatures.

intensity of band II due to radiative transitions of π^*-UP transitions of N_2 increases. This leads to change in the position of the intensity maximum in the PL spectrum observed at room temperature 300 K, which moves into the region of lower energies.

The material synthesized at the higher temperature of 600°C differs in structure and composition. When the synthesis temperature is raised the degree of polymerization of the g-C_3N_4 rises, and the concentration of oxygen is increased. The oxygen can then enter at the crystal lattice sites of the semiconductor and distort it. Thermal stratification of the individual layers of the g-C_3N_4 can also occur. These factors change the energy structure of the semiconductor and actually increase the width of the forbidden band [3, 12, 29, 30]. The maxima of the PL bands that can be identified in the spectrum of the g-C_3N_4 sample obtained at 600°C are therefore shifted into the region of higher energies compared with the analogous bands observed for the samples synthesized at 500°C. Since the degree of polymerization of the material obtained at 600°C is higher the intensity of band II due to the π levels increases. Also activated at room temperature are the levels corresponding to the nitrogen defects, the concentration of which in the material obtained at the higher temperature is higher because of the start of thermal decomposition, leading to increase in the intensity of the corresponding band III, which becomes readily visible in the measurements made at 300 K. In other words the maximum of the whole PL spectrum of the sample undergoes a "red" shift similar to what occurs when the length of the process at the lower synthesis temperature of 500°C is increased and is due to redistribution of the intensity of the individual components of its bands.

The appearance of an additional PL band with a maximum at 3.074 eV is due to a σ^*–σ transition. It is obvious that the probability of such a radiative process in this case increases with decrease in the temperature of the sample. This process may also be due to transition of electrons from other energy levels (π^* or those due to defects at the nitrogen) to the σ level.

Conclusions. Investigation of the photoluminescence of graphitized carbon nitride, synthesized by pyrolytic decomposition of melamine followed by thermal polymerization and condensation at various temperatures and process times, over a wide range of temperatures (10–300 K) showed that the structure of semiconducting g-C_3N_4 can be controlled by changing not only the synthesis temperature but also the length of the process. The photoluminescence spectrum of the synthesized g-C_3N_4 consists of bands due to radiative transitions between excited σ and π bonds to the energy levels of the unshared electron pairs of the nitrogen atom and oxygen impurity atoms and also structural defects due to nitrogen and oxygen impurity atoms. The degree of polymerization of g-C_3N_4 is increased by increasing the length of the synthesis process at 500°C and also by raising the synthesis temperature to 600°C. However, by using the process at the lower temperature it is possible to avoid thermal stratification and decomposition of g-C_3N_4, which has already begun at 600°C. Increase of the degree of polymerization leads to a shift of the position of the maximum in the photoluminescence spectrum into the region of smaller energies as a result of the formation of a larger amount of π bonds between the carbon atom and nitrogen with sp^2 hybridization, forming a system with a smaller forbidden band width. However, the energy of each of the permitted radiative transitions between the levels in the material synthesized at the higher temperature (600°C) is somewhat higher on account of increase in the forbidden band width. This is due to stratification of the g-C_3N_4, entry of a larger amount of oxygen at the crystal lattice sites, and thermal decomposition of the semiconductor.

The results from control of the luminescence characteristics of g-C_3N_4 can be used in the creation of light-emitting and photovoltaic instruments and also in the development of composite heterostructures for photocatalytic coatings.

Acknowledgments. The work was carried out for GPNI Republic of Belarus "Conference-2020" (assignment 3.05), GPNI Republic of Belarus "Material Behavior and Materials Technology" (assignment 1.56) with a grant from the Ministry of Education, Republic of Belarus, for doctoral candidates.

The authors express their gratitude to V. V. Uglov for the x-ray structural analysis and to D. V. Zhigulin for x-ray energy dispersive analysis of the samples.

REFERENCES

1. Y. Zheng, L. Lin, B. Wang, and X. Wang, *Angew. Chem., Int. Ed.*, **54**, 12868–12884 (2015).
2. E. Kroke, M. Schwarz, E. Horath-Bordon, P. Kroll, B. Noll, and A. D. Norman, *New J. Chem.*, **26**, 508–512 (2002).
3. A. Wang, C. Wang, L. Fu, W. Wong-Ng, and Y. Lan, *Nano-Micro Lett.*, **9**, 47 (2017).
4. B. Molina and L. E. Sansores, *Mod. Phys. Lett. B*, **13** (1999) 193–201 (2017).
5. Y. Zhao, J. Zhang, and L. Qu, *Chem. Nano. Mat.*, **1**, 298–318 (2015).
6. A. Zambon, J.-M. Mouesca, C. Gheorghiu, P.A. Bayle, J. Pécaut, M. Claeys-Bruno, S. Gambarelli, and L. Dubois, *Chem. Sci.*, **7**, 945–950 (2016).
7. A. Thomas, A. Fischer, F. Goettmann, M. Antonietti, J.-O. Müller, R. Schlögl, and J. M. Carlsson, *J. Mater. Chem.*, **18**, 4893–4908 (2008).
8. J. Wen, J. Xie, X. Chen, and X. Li, *Appl. Surf. Sci.*, **391**, 72–123 (2017).
9. J. Hernández-Torres, A. Gutierrez-Franco, P. G. González, L. García-González, T. Hernandez-Quiroz, L. Zamora-Peredo, V. H. Méndez-García, and A. Cisneros-de la Rosa, *J. Spectrosc.*, **2016**, 5810592 (2016),
10. J. Zhu, P. Xiao, H. Li, and S. A. C. Carabineiro, *ACS Appl. Mater. Interf.*, **6**, 16449–16465 (2014).
11. W.-J. Ong, L.-L. Tan, Y. H. Ng, S.-T. Yong, and S.-P. Chai, *Chem. Rev.*, **116**, 7159–7329 (2016).
12. A. Sudhaik, P. Raizada, P. Shandilya, D.-Y. Jeong, J.-H. Lim, and P. Singh, *J. Ind. Eng. Chem.*, **67**, 28–51 (2018).
13. X. Wang, K. Maeda, A. Thomas, K. Takanabe, G. Xin, J. M. Carlsson, K. Domen, and M. Antonietti, *Nat. Mater.*, **8**, 76–80 (2009).
14. B. Jürgens, E. Irran, J. Senker, P. Kroll, H. Müller, and W. Schnick, *J. Am. Chem. Soc.*, **125**, 10288–10300 (2003).
15. M. J. Bojdys, J.-O. Müller, M. Antonietti, and A. Thomas, *Chem. Eur. J.*, **14**, 8177–8182 (2008).
16. W. Wu, J. Zhang, W. Fan, Z. Li, L. Wang, X. Li, Y. Wang, R. Wang, J. Zheng, M. Wu, and H. Zeng, *ACS Catal.*, **6**, 3365–3371 (2016).
17. Y. Zhang, Q. Pan, G. Chai, M. Liang, G. Dong, Q. Zhang, and J. Qiu, *Sci. Rep.*, **3**, 1943 (2013).
18. S. Yin, J. Han, T. Zhoua, and R. Xu, *Catal. Sci. Technol.*, **5**, 5048–5061 (2015).
19. B. Choudhury, K. K. Paul, D. Sanyal, A. Hazarika, and P. K. Giri. *J. Phys. Chem. C*, **122**, 9209–9219 (2018).
20. D. Das, D. Banerjee, D. Pahari, U. K. Ghorai, S. Sarkar, N. S. Das, and K. K. Chattopadhyay, *J. Lumin.*, **185**, 155–165 (2017).
21. N. M. Denisov, E. B. Chubenko, V. P. Bondarenko, and V. E. Borisenko, *Tech. Phys. Lett.*, **45**, 108–110 (2019).
22. E. B. Chubenko, A. V. Baglov, E. S. Lisimova, and V. E. Borisenko, *Int. J. Nanosci.*, **18**, 1940042 (2019).
23. G. Zhang, J. Zhang, M. Zhang, and X. Wang, *J. Mater. Chem.*, **22**, 8083–8091 (2012).
24. Z. Gan, Y. Shen, J. Chen, Q. Gui, Q. Zhang, and S. Nie, *Nano Res.*, **9**, 1801–1812 (2016).
25. D. Das, S. L. Shinde, and K. K. Nanda, *ACS Appl. Mater. Interf.*, **83**, 2181–2186 (2016).
26. Y. P. Varshni, *Physica*, **34**, 149–154 (1967).
27. J. Fu, B. Zhu, C. Jiang, B. Cheng, W. You, and J. Yu, *Small*, **13**, 1603938 (2017).
28. Y. Jiang, Z. Sun, C. Tang, Y. Zhou, L. Zeng, and L. Huang, *Appl. Catal. B*, **240**, 30–38 (2019).
29. F. Dong, Y. Li, Z. Wang, and W. K. Ho, *Appl. Surf. Sci.*, **358**, 393–403 (2015).
30. J. Bian, C. Huang, and R.-Q. Zhang, *Chem. Sus. Chem.*, **9**, 1–14 (2016).